

Development of a Dynamic Model of Thermal Processes for Plasma Surfacing at Direct and Reverse Polarity

¹Sergey Dmitrievich Neulybin, ²Gleb Lvovich Permyakov, ³Dmitriy Nikolayevich Trushnikov, ⁴Yuri Dmitrievich Shchitsyn, ⁵Vladimir Yakovlevich Belenkiy

^{1,2,3,4,5}Department for Welding Production, Metrology and Technology of Materials,
Perm National Research Polytechnic University, Perm, Russian Federation

Orcid Id: 0000-0002-8791-1696

Abstract

The article investigates multilayer plasma surfacing at direct and reverse polarity. The article describes the main provisions in the field of additive production using various technologies. The use of a plasma heating source is shown to have a number of advantages both from technological and economic points of view. A technique is developed and a mathematical description of the heating source is presented with taking into account the heat transfers from plasma flow and near-electrode processes. A three-dimensional model of heat transfer into the workpiece for plasma surfacing at direct and reverse polarity is developed. The numerical implementation of the process for 10Cr18Ni10Ti steel was carried out. Standard deviation in the test samples did not exceed 10%.

Keywords: Additive technologies, multiplayer surfacing, plasma torch, numerical simulation, finite-elements method, high alloy steel

INTRODUCTION

Additive and hybrid technologies are the key components for building up the digital economy of the 21st century. Simultaneously, until recently, when speaking about additive technologies, basically the complex-shaped small-sized products production is meant [1, 2, 3, 4]. Forming layered materials using electric arc as a heat source and a filler wire consumables contributes to increased productivity in forming of billets [5, 6, 7, 8, 9]. Reducing the technological preparation costs of production increases the utilization factor of the material and provides for getting finished products with specified performance characteristics. Using of dissimilar materials in one billet ensures an increase in the load-bearing capacity of the structure as a whole and gives special properties to the working surfaces.

Despite the development of 3D surfacing methods in recent years [10, 11], the problems of lowering heat input to the product when applying layers, increasing layers adhesion, possibility to process materials of different classes, reducing defectiveness of clad metal, providing the required properties are still acute [12]. The structure and properties of multi-layer materials are largely determined by the peculiarities of heat transfer to the product at cladding. Using highly concentrated energy sources allows reducing heat input to the product and

improve the conditions to form the structure and properties of multi-layer materials. The use of plasma technologies to form layered materials has several advantages from the technological and economic points of view.

Production of layered materials may involve alloy steels and non-ferrous metal alloys with different heat-transfer properties. In addition, at continuous multilayer surfacing, the temperature fields overlap from layer to layer affecting the formation of the final structure and properties of the resulting materials.

The development of technology and its distribution to various groups of materials requires formalization of the investigated processes of additive formation of the billet, by means of reflowing of the filler wire material in the form of a mathematical description of the processes. Applying mathematical simulation along with computational experiment contributes to a better understanding of the ongoing physical processes and obtaining additional information on the realizable superimposition of thermal cycles.

Analytic and numerical methods are used to solve heat conductivity problems. Existing analytical methods allow for obtaining solutions only for processes described by linear differential equations under linear boundary conditions, i.e. for those cases when the heat-transfer properties can be considered independently of temperature. Analytical methods lead to general equations of processes valid for various numerical values of the parameters characterizing the given problem: geometric dimensions, heat characteristics of heating mode and physical properties of metals. The simplest problems allow for obtaining a solution in a closed form, i.e. expressing the process equation through known functions of time, spatial coordinates and constant process parameters. In more complicated problems, solutions are described by definite integrals or infinite series [13, 14, 15].

Numerical methods, unlike analytical, allow for solving heat conductivity problem in a complex formulation, i.e. considering the real geometry of the structure, temperature dependence of heat-transfer properties, heating source distribution, etc., which makes their application the only possible solution under the conditions of simulating the cladding process. Currently, the most common and widespread in commercial software packages is the finite-

element method (FEM). Modern software products, e.g. ANSYS, COMSOL provide broad opportunities for solving the problem of heat and mass transfer while welding [16, 17, 18, 19, 20, 21, 22].

The paper presents the results of simulating heat processes at plasma surfacing at direct and reverse polarity. The article also analyses physical effects arising from plasma surfacing. The work substantiates correctness of the assumptions and approaches to developing the mathematical model of the process. The article determines influence of current polarity and process parameters of plasma surfacing on heat transfer into the workpiece and heat contact area of plasma arc with the workpiece. The authors propose an algorithm for numerical implementation of the mathematical model of heat processes for plasma surfacing at direct and reverse polarity. Also, the authors verify them for 10Cr18Ni10Ti steel.

Until now, all the results of plasma surfacing/welding simulation with reverse polarity were ignore wandering of cathode spots over workpiece surface. Complete dynamic models considering this phenomenon are not available up to now.

METHODS

Mathematical formulation of the problem requires known heat input to the product from plasma arc at direct and reverse polarity, as well as heat transfer fraction distribution from the plasma jet(plasma flow) and electrode spots. Heat transfer to the product at compressed plasma arc of direct action is performed by two mechanisms: convection from the plasma jet and heat input to active (electrode) spots. The works by [23] found out that at same current and other equal conditions, heat input at plasma torch work at reverse polarity to the product is 1.3...1.6 times higher than at direct polarity, which is explained by the higher voltage at the arc. The work shows that, in contrast to a compressed direct polarity arc, a compressed reverse polarity arc is characterized by a more even distribution of heat power over the product surface (Figure 1).

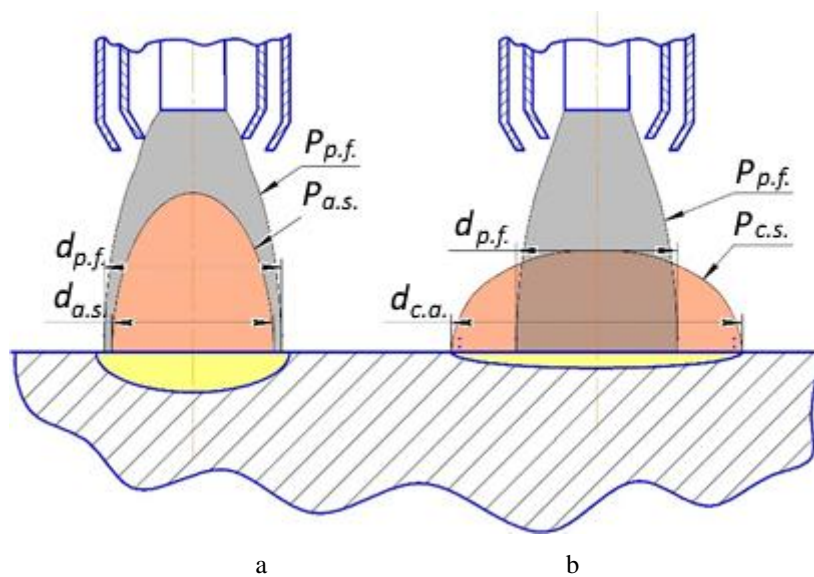


Figure 1: Heat transfer to the workpiece at plasma processing.
 (a) direct polarity, (b) reverse polarity.

$P_{p.f.}$ is power transmitted by convection, $P_{a.s.}$ is power released in anode spot, $P_{c.s.}$ is power released in cathode area, $d_{p.f.}$ is plasma flow diameter, $d_{a.s.}$ is anode spot diameter, $d_{c.a.}$ is cathode area diameter

At plasma processing at direct polarity, $d_{p.f.}$ and $d_{a.s.}$ are proportional and it is impossible to control their size separately. At plasma processing at reverse polarity, the arc belongs to the type of arcs with nonstationary cathode spots wandering along its surface. The width of wandering depends on the design of the plasma torch and the product material.

One of the distinguishing features of nonstationary spots is the short duration of their existence and the high current density in them ($j \sim 10^5 \dots 10^6 \text{ A/m}^2$), while the specific heat flows reach values of ($q \sim 10^6 \dots 10^7 \text{ W/cm}^2$) (Figure 2), and with values of $d_{p.f.}$ And $d_{c.a.}$ can be actively managed and regulated separately.

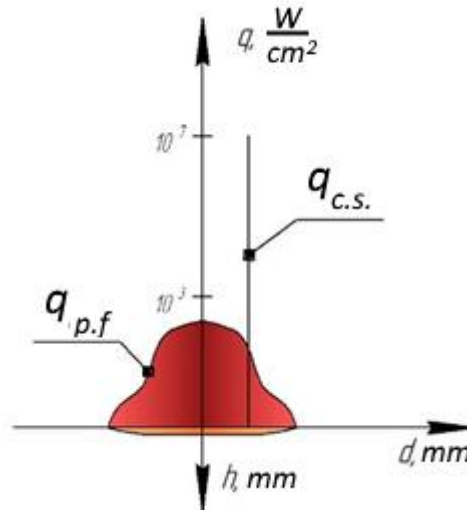


Figure 2: The peculiarity of heat transfer to the workpiece at plasma torch operation at reverse polarity. $q_{c.s.}$ is heat flow from a non-permanent cathode spot, $q_{p.f.}$ is resulting transfer duty, d is heat transfer diameter, h is workpiece penetration depth

In continuation of the studies presented in the works on estimating the share of heat transfer to the workpiece [23, 24, 25, 26] based on regression equations (1), (2), (3) presented below, a dynamic model of heat transfer to the product was developed for plasma surfacing at direct and reverse polarity and its numerical implementation for 10Cr18Ni10Ti steel.

$$P_{wdp} = 170.45 + 18.5I_d + 227.8Q_p - 311.1d_c, \quad (1)$$

$$P_{wrp} = 886.9 + 20.4I_d + 364.6Q_p - 510.1d_c, \quad (2)$$

$$P_{wrppj} = 886.9 + 15.34I_d + 367.7Q_p - 510.1d_c, \quad (3)$$

where P_{wdp} is power input into workpiece at direct polarity, P_{wrp} is power input into workpiece at reverse polarity, P_{wrppj} is power transferred to the workpiece by plasma jet at reverse polarity.

MATHEMATICAL MODEL

The model is based on the solution of heat problem of melting welding consumables by a plasma arc in a three-dimensional setting. Basic equations for calculations are in [17, 18, 19, 20, 21, 22].

Plasma surfacing mathematical model is based on solving the differential heat conductivity equation with moving coordinates (energy transfer equation):

$$\frac{\partial T}{\partial t} = a \cdot \left(\frac{\partial^2 T}{\partial x^2} + \frac{\partial^2 T}{\partial y^2} + \frac{\partial^2 T}{\partial z^2} \right) + V \frac{\partial T}{\partial x} + \frac{P}{C_{eff} \rho}, \quad (4)$$

where T is temperature, a is heat diffusivity, and V is medium (coincides with plasma torch velocity in area 1 in Figure 4 and wire feed speed velocity in area 2), ρ is density. Convective transfer input to melted materials is considered by the formula $\lambda_{eff} = \lambda_L (2 - T_L / T)$, where λ_L is

liquid heat conductivity coefficient, and T_L is liquidus temperature.

Internal melting and crystallization heat was considered by introducing an effective heat capacity:

$$C_{eff} = C_0 + \frac{\exp[-((T - T_{melt}) / (T_L - T_S))^2]}{\sqrt{\pi} (T_L - T_S)} H_f, \quad (5)$$

where C_0 is heat capacity depending on temperature, H_f is internal melting heat, T_{melt} is melting point assumed to be the median in the range from solidus temperature T_S to liquidus T_L .

Heat transfer into the product at using plasma torch from plasma flow and near-electrode processes can be represented as follows:

$$q = q_{p.f.} + q_{c.s.}, \quad (6)$$

$$q_{p.f.} = \frac{k_{p.f.} P}{2\pi \cdot R_{p.f.}^2} \exp\left(-\frac{2 \cdot R_{p.f.}^2}{R_{p.f.}^2}\right), \quad (7)$$

$$q_{c.s.} = \frac{k_{c.s.} P}{2\pi \cdot r_{c.s.}^2} \exp\left(-\frac{2 \cdot r_{c.s.}^2}{r_{c.s.}^2}\right), \quad (8)$$

where q is heat flow supplied to the product by plasma arc; $q_{p.f.}$ is heat flow supplied by plasma flow; $q_{c.s.}$ is heat flow, reflecting cumulative heat effect of cathode spots (for welding at direct polarity $k_{c.s.} = 0$); $k_{p.f.}$, $k_{c.s.}$ are coefficients considering power distribution between plasma flow and cathode spots, respectively ($k_{p.f.} + k_{c.s.} = 1$), are calculated using statistical sub-model described by equations

(1), (2), (3); plasma flow is described by a circle with a radius of $R_{p.f.} = \sqrt{x^2 + y^2}$ centered at the origin of coordinates; cathode spots are described by circles of radius of $r_{c.s.} = \sqrt{(x - x_0)^2 + (y - y_0)^2}$ with centers in coordinates x_0, y_0 , determined randomly, using the built-in function $random(x_0(t), y_0(t))$.

The problem was solved in a three-dimensional setting. Due to the symmetry, the description is satisfied with inclusion of only a half of the entire object in the computational space. Differential energy transfer equation is a mathematical model of a whole class of heat conductivity phenomena and has an infinite set of solutions. It is necessary to have additional data not contained in the original differential equation to obtain one particular solution characterizing a particular process from this set. These additional conditions, determining together with the differential equation the particular problem, are called single-valuedness conditions. Single-valuedness conditions include geometric conditions, physical properties of the body, boundary and initial conditions.

The boundary conditions of mixed type were used. On the processed surface of the product:

$$\lambda \frac{\partial T}{\partial z} = q_{p.f.} + q_{c.s.} - \alpha_0(T - T_0), \quad (9)$$

in the symmetry plane:

$$\lambda \frac{\partial T}{\partial n} = 0, \quad (10)$$

and on all other surfaces:

$$\lambda \frac{\partial T}{\partial n} = -\alpha_0(T - T_0), \quad (11)$$

α_0 is effective heat-transfer coefficient, considering heat loss for convection and radiation.

Welding bead shape was approximated by a half-ellipse. Welding bead volume for a unit of time coincides with the supplied welding material volume $\pi \cdot r_{fw}^2 V_{fw} = \pi \cdot a_e b_e V_{pl} / 2$, where a_e, b_e are width and height of the welding bead, respectively. Welding bead width a_e is determined by the successive approximation method from the condition of its equality to width.

NUMERICAL IMPLEMENTATION

Numerical implementation was carried out using Comsol 4.4 software package (Heat Transfer module). Computational space geometry is shown in Figure 3.

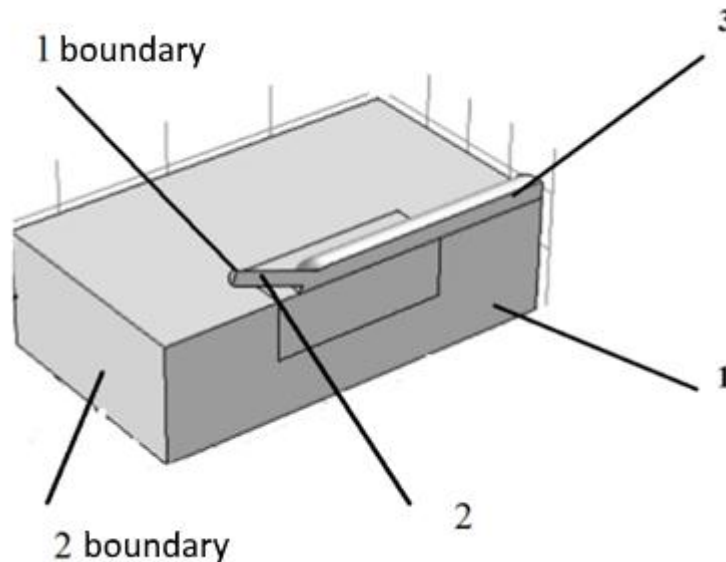


Figure 3: Plasma surfacing computational scheme. 1 is a workpiece, 2 is filler wire, 3 is weld bead

Process simulation area was covered with a three-dimensional grid inscribed in the computational space. Computational space dimensions are 70x30x10 mm. The

grid had an uneven step (Figure 4). The maximum cell size in the arc impact zone and welding wire feed constituted 0.5 mm, and in the remaining space is 2.5 mm.

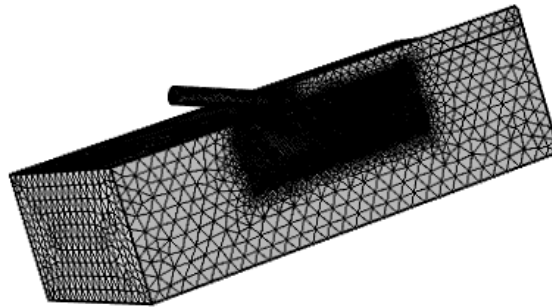


Figure 4: Splitting computational space into a grid

The initial calculation parameters included material heat-transfer properties. The latter are given in Table 1 as well as surfacing mode parameters from Table 2.

Table 1: Heat-transfer properties of the clad material taken at calculation

Characteristic	Designation	Dimension	Value
Liquidus temperature	T_L	[°C]	1450
Solidus temperature	T_S	[°C]	1520
Specific heat capacity	C	[J·kg ⁻¹ ·K ⁻¹]	500
Density	ρ	[kg·m ⁻³]	7680
Heat conductivity	λ	[W·m ⁻¹ ·K ⁻¹]	28.9
Specific melting heat	H_f	kJ/kg	84

Table 2: Plasma surfacing mode

Sample No.	I_a , A	G_p , l/min	G_p , l/min	V_{pl} , m/h	V_{fw} , m/h
1	80	3.8	5.5	12	36

Solution of heat processes dynamic model at reverse polarity considering non-permanent cathode spots impact is shown in Figure 5.

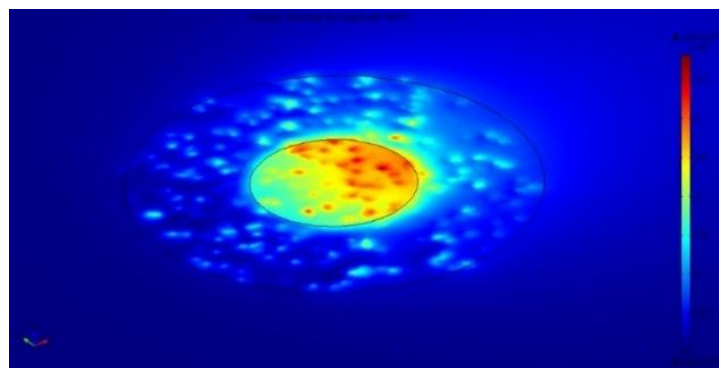


Figure 5: Power density distribution under plasma arc reverse polarity impact considering non-permanent cathode spots impact

Since reducing heat input to the product is important in producing multi-layer materials, information about heat situation on the product surface is important. Calculated thermal cycle makes it possible to determine the nature and degree of phase transformations completeness and to predict

the final structure and properties of the material. Thermal cycle of plasma surfacing at direct and reverse polarity are built (Figure 6) to explain the mechanism of structure formation

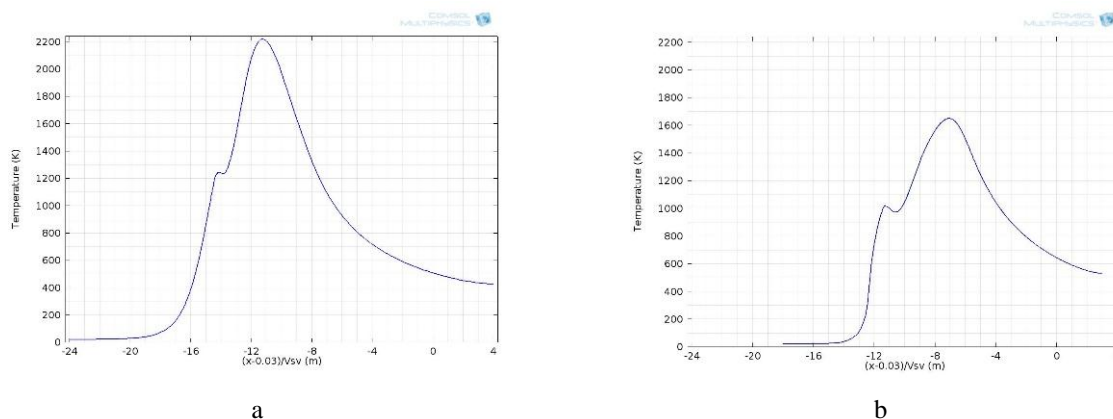


Figure 6: Thermal cycle of heating-cooling of the surface while surfacing at direct (a) and reverse polarity (b)

Thermal cycle analysis allows to conclude that reverse polarity at surfacing provides for the necessary and sufficient conditions for high-quality fusion of the material, while metal dwell time above crystallization temperatures is significantly reduced. It happens because of the rapid

heating and melting of metal in thin surface layer, under the influence of non-permanent cathode spots.

Heat transfer problem solution and comparison with the experimental data was carried out at the example of plasma surfacing of a 10Cr18Ni10Ti steel filler wire onto the sample of the same material (Figure 7).



Figure 7: Experimental and calculated cross-sections of the weld bead in plasma surfacing at direct (a) and reverse polarity (b)

CONCLUSIONS

1. Statistical data analysis of heat transfer values to the product was carried out under various operating conditions of plasma torch at direct and reverse polarity. Regression equations are obtained, which allows for estimating the share of heat transfer to the product from plasma flow and near-electrode processes.
2. Mathematical models of plasma surfacing at direct and reverse polarity are developed considering heat transfer into the product from the near-electrode processes.
3. Numerical implementation and mathematical models verification of plasma surfacing at direct and reverse polarity were carried out considering the local effect of non-permanent cathode spots for 10Cr18Ni10Ti steel.
4. The developed models allow for estimating weld bead geometrical parameters, surfacing heat cycles, and for making a preliminary choice of technological parameters of surfacing. The deviation in the test examples did not exceed 10% for the height and width

of welding bead and 20% for determining the depth of welding at reverse polarity.

ACKNOWLEDGMENTS

This work was carried out with financial supported by the Ministry of Education and Science of the Russian Federation (RFMEFI58317X0062) within the framework of the BRICS project.

REFERENCES

- [1] Elliott, J. A., 2011, "Novel Approaches to Multiscale Modelling in Materials Science", *International Materials Reviews*, 56(4), pp. 207-225. DOI: <http://dx.doi.org/10.1179/1743280410Y.0000000002>
- [2] Petrick, I., Simpson, T., 2013, "3D Printing Disrupts Manufacturing", *Research-Technology Management*, 56(6), pp. 15-16. DOI: 10.5437/08956308X5606193
- [3] Morrow, W. R., Qi, H., Kim, I., Mazumder, J., and Skerlos, S. J., 2007, "Environmental Aspects of Laser-Based and Conventional Tool and Die

- Manufacturing”, *Journal of Cleaner Production*, 15(10), pp. 932-943. DOI: <https://doi.org/10.1016/j.jclepro.2005.11.030>
- [4] Wray, P., 2014, “Additive Manufacturing: Turning Manufacturing Inside Out”, *American Ceramic Society Bulletin*, 93(3), pp. 17-23.
- [5] Jhavar, S., Jain, N. K., Paul, C. P., 2014, “Development of micro-plasma transferred arc (μ -PTA) wire deposition process for additive layer manufacturing applications”, *Journal of Materials Processing Technology*, 214(5), pp. 1102-1110. DOI: <https://doi.org/10.1016/j.jmatprotec.2013.12.016>
- [6] Freedman, D. H., 2012, “Layer by Layer”, *Technology Review*, 115, pp. 50-53.
- [7] Qi, H. B., Yan, Y. N., Lin, F., He, W., Zhang, R. J., 2006, “Direct metal part forming of 316L stainless steel powder by electron beam selective melting”, *Proceedings of the Institution of Mechanical Engineers, Part B: Journal of Engineering Manufacture*, 220(11), pp. 1845-1853. DOI: <https://doi.org/10.1243/09544054JEM438>
- [8] Murr L. E., Gaytan, S. M., Ramirez, D. A., Martinez, E., Hernandez, J., Amato, K. N., Shindo, P. W., Medina, F. R., Wicker, R. B., 2012, “Metal fabrication by additive manufacturing using laser and electron beam melting technologies”, *Journal of Materials Science & Technology*, 28(1), pp. 1-14. DOI: [https://doi.org/10.1016/S1005-0302\(12\)60016-4](https://doi.org/10.1016/S1005-0302(12)60016-4)
- [9] Frazier, W. E., 2014, “Metal Additive Manufacturing: A Review”, *Journal of Materials Engineering Performance*, 23(6), pp. 1917-1928. DOI: <https://doi.org/10.1007/s11665-014-0958-z>
- [10] Kapil, S., Legesse, F., Kulkarni, P., Joshi, P., Desai, A., Karunakaran, K. P., 2016, “Hybrid Layered Manufacturing using Tungsten Inert Gas Cladding”, *Progress in Additive Manufacturing*, 1(1-2), pp. 79-91. DOI <https://doi.org/10.1007/s40964-016-0005-8>
- [11] Zhang, Y., Bernard, A., Harik, R., Karunakaran, K. P., 2017, “Build Orientation Optimization for Multi-Part Production in Additive Manufacturing”, *Journal of Intelligent Manufacturing*, 28(6), pp. 1393-1407. DOI <https://doi.org/10.1007/s10845-015-1057-1>
- [12] Shchitsyn, Yu. D., Kosolapov, O. A., Shchitsyn, V. Yu., 2010, “Capabilities of plasma metal processing at reverse polarity”, *Welding and Diagnostics*, 3, pp. 43-45.
- [13] Yazovskikh, V. M., 2008, *Mathematical Simulation and Engineering Methods of Calculation in Welding: in 2 parts. Part 2. Heat Processes at Welding and Simulation in the MathCad Package*, Perm State Technical University, Perm, Russia.
- [14] Rykalin, N. N., 1951, *Calculations of Heat Processes at Welding*, Mashgiz, Moscow, Russia.
- [15] Karkhin, V. A., 2015, *Heat Processes at Welding*, Publishing house of the Polytechnic University, St. Petersburg, Russia.
- [16] Musin, R. A., Trushnikov, D. N., Shkurikhin, V. A., Putin, Yu. A., 2010, “Mathematical simulation of welding processes in the Femlab 3.0 package”, *Bulletin of Perm National Research Polytechnic University*, 12(4), pp. 7-16.
- [17] Brent, A. D., Voller, V. R., and Reid, K. J., 1988, “Enthalpy-porosity technique for modeling convection-diffusion phase change: Application to the melting of a pure metal”, *Numerical Heat Transfer*, 13(3), pp. 297-318. DOI: <http://dx.doi.org/10.1080/10407788808913615>
- [18] Kou, S., and Sun, D. K., 1985, “Fluid flow and weld penetration in stationary arc welds”, *Metallurgical Transactions A*, 16(2), pp. 203-213. DOI: <https://doi.org/10.1007/BF02816047>
- [19] [19] Kim, C. H., Zhang, W., and DebRoy, T., 2003, “Modeling of temperature field and solidified surface profile during gas metal arc fillet welding”, *Journal of Physics*, 94(4), pp. 2667-2679. DOI: <http://dx.doi.org/10.1063/1.1592012>
- [20] De, A., and DebRoy, T., 2004, “Probing unknown welding parameters from convective heat transfer calculation and multivariable optimization”, *Journal of Physics D: Applied Physics*, 37(1), pp. 140-150. DOI: <http://dx.doi.org/10.1088/0022-3727/37/1/023>
- [21] De, A., and DebRoy, T., 2004, “A smart model to estimate effective heat conductivity and viscosity in weld pool”, *Journal of Applied Physics*, 95(9), pp. 5230-5240. DOI: <http://dx.doi.org/10.1063/1.1695593>
- [22] Rappaz, M., Bellet, M., Deville, M., 2003, *Numerical Modeling in Materials Science and Engineering*, Springer, Berlin, Germany.
- [23] Shchitsyn, V. Yu., Yazovskikh, V. M., 2002, “Influence of polarity on heat input to plasma torch nozzle”, *Welding Production*, 1, pp. 17-19.
- [24] Shchitsyn, Yu. D., Kosolapov, O. A., Strukov, N. N., 2010, “Energy distribution of the compressed arc at plasma torch at reverse polarity”, *Welding and Diagnostics*, 3, pp. 13-16.
- [25] Kuchev, P. S., Shchitsyn, Yu. D., Belinin, D. S., Shilov, A. Yu., 2013, “Heat characteristics for single-

- arc and combined work mode of a plasma torch”,
Welding. Renovation. Triboengineering, pp. 46-49.
- [26] Schitcyn, Y. D., Belinin, D. S., Neulybin, S. D.,
Gilev, I. A., Panov, A. I., 2015, “Determination of
voltage drop across the anode area arc plasma
processing of metals ”, Bulletin of Perm National
Research Polytechnic University, 17(2), pp. 5-12.